ELSEVIER

Journal of Contaminant Hydrology 48 (2001) 277–304

JOURNAL OF Contaminant Hydrology

www.elsevier.com/locate/jconhyd

On the selection of primary variables in numerical formulation for modeling multiphase flow in porous media

Yu-Shu Wu [a,*], Peter A. Forsyth [b]

[a] *Earth Sciences Division, Lawrence Berkeley National Laboratory, MS 90-1116, One Cyclotron Road, Berkeley, CA 94720, USA*

[b] *Department of Computer Sciences, University of Waterloo, Waterloo, Ontario, Canada N2L 3G1*

Received 28 September 1999; received in revised form 16 September 2000; accepted 6 October 2000

Abstract

Selecting the proper primary variables is a critical step in efficiently modeling the highly nonlinear problem of multiphase subsurface flow in a heterogeneous porous-fractured media. Current simulation and ground modeling techniques consist of (1) spatial discretization of mass and/or heat conservation equations using finite difference or finite element methods; (2) fully implicit time discretization; (3) solving the nonlinear, discrete algebraic equations using a Newton iterative scheme. Previous modeling efforts indicate that the choice of primary variables for a Newton iteration not only impacts computational performance of a numerical code, but may also determine the feasibility of a numerical modeling study in many field applications. This paper presents an analysis and general recommendations for selecting primary variables in simulating multiphase, subsurface flow for one-active phase (Richards' equation), two-phase (gas and liquid) and three-phase (gas, water and nonaqueous phase liquid or NAPL) conditions. In many cases, a dynamic variable switching or variable substitution scheme may have to be used in order to achieve optimal numerical performance and robustness. The selection of primary variables depends in general on the sensitivity of the system of equations to the variables selected at given phase and flow conditions. We will present a series of numerical tests and large-scale field simulation examples, including modeling one (active)-phase, two-phase and three-phase flow problems in multi-dimensional, porous-fractured subsurface systems.

Keywords: Multiphase flow simulation; Newton iteration; Primary variable selection; Variable substitution; Richards' equation and unsaturated flow

* Corresponding author. Tel.: +1-510-486-7291; fax: +1-510-486-5686.
E-mail address: yswu@lbl.gov (Y.-S. Wu).

0169-7722/01/$ - see front matter
PII: S0169-7722(00)00180-7

1. Introduction

Even with the continual progress made in both computational algorithms and computer hardware, numerical simulation of multiphase subsurface flow remains a challenging task. Flow of two- or three-phase fluids in the subsurface results in a highly nonlinear, difficult problem and in general extensive computational resources are needed. In the past few decades, modeling multiphase flow through porous or fractured porous media has received increasing attention because of its importance in the areas of underground natural resource recovery, waste storage, soil physics, and environmental remediation. Since the late 1950s, significant progress has been made in developing and applying numerical simulation techniques in petroleum engineering (Coats, 1987; Aziz and Settari, 1979; Peaceman, 1977; Thomas, 1982) and groundwater literature (Huyakorn and Pinder, 1983; Istok, 1989). Despite these advances, modeling the coupled processes of multiphase fluid flow in a heterogeneous porous medium remains a conceptual and mathematical challenge. The difficulty stems from the nature of the inherent nonlinearity and poorly determined constitutive relations for multiphase flow, as well as the computational requirements for a field application. Numerical modeling approaches currently used for simulating those coupled multiphase processes are generally based on methodologies developed for petroleum and geothermal reservoir simulations. They involve solving fully coupled formulations describing these processes using finite-difference or finite-element schemes with a volume averaging approach.

Earlier research on modeling multiphase flow in porous media was initially carried out for the development of petroleum (Douglas et al., 1959; Peaceman and Rachford, 1962; Coats et al., 1967) and geothermal reservoirs (Mercer et al., 1974; Thomas, 1978; Pruess, 1987). More recently, problems involving unsaturated and two-phase flow in aquifers and soils were increasingly recognized and studied in hydrology and soil science. Many numerical approaches were developed (e.g., Narasimhan and Witherspoon, 1976; Cooley, 1983; Huyakorn et al., 1984; Morel-Seytoux and Billica, 1985; Cella et al., 1990) for modeling flow and transport phenomena in the vadose zone (Gee et al., 1991).

While there has been an ongoing interest in understanding multiphase flow processes using a numerical approach in different disciplinary areas, in recent years soil and groundwater contamination by nonaqueous phase liquids (NAPL), such as contaminants from oil and gasoline leakage, or other organic chemicals, has received increasing attention. The NAPL-related environmental concern has motivated research activities in developing and applying multiphase flow and transport models for assessing NAPL contamination and the associated clean up operations. As a result, many numerical models and computational algorithms have been developed and improved for solving multiphase fluid flow and organic-chemical transport problems in the vadose zone, porous, and fractured media (Abriola and Pinder, 1985; Faust, 1985; Forsyth, 1988; 1991, 1994; Forsyth and Shao, 1991; Kaluarachchi and Parker, 1989; Falta et al., 1992a,b; Huyakorn et al., 1994; Panday et al., 1994; Wu et al., 1994; Kuiper and Illangasekare, 1998). Numerical modeling approaches have become standard techniques in investigating subsurface NAPL contamination and implementing remediation measures.

In general, the numerical techniques used for modeling multiphase subsurface flow consist of (1) spatial discretization of mass conservation equations using finite-difference or finite-element schemes; (2) fully implicit time discretization; (3) iterative approaches, such as the Newton iteration, to solve nonlinear, discrete algebraic equations. The previous studies of modeling multiphase flow through porous media (e.g., Wu et al., 1992; Forsyth et al., 1995, 1998; Forsyth, 1994) have identified that choice of the primary variables for a Newton iteration has a significant impact on computational performance of a multiphase model. However, little investigation has been carried out regarding the general strategy and selection of primary variables in modeling multiphase flow and transport processes.

This paper presents a comparative analysis and general recommendations for selecting primary variables in simulating: (1) one phase flow (solving Richards' equation); (2) two-phase (gas and liquid) flow; and (3) three-phase (gas, water and NAPL) flow. We present and discuss a general, mass-conservative model formulation for a control-volume discretization and perform a series of numerical tests using large-scale field simulation examples, including modeling one-phase, two-phase and three-phase flow problems in multi-dimensional, heterogeneous fractured rocks. In all the cases of solving Richards' equation for one-active-phase flow, two-phase (gas and water) flow, and three-phase (gas, water and NAPL) flow, the fully implicit approach is used and tested.

This study indicates that use of proper primary variables is a critical step in efficiently modeling highly nonlinear multiphase subsurface flow problems in heterogeneous porous and fractured media. The optimal selection of primary variables depends, in general, on the particular problem being simulated. In some circumstances, the selection of primary variables has a large effect on the conditioning of the Jacobian matrix and hence a large effect on the number of Newton iterations (and the number of iterations required to solve the Jacobian system). In formulating a multiphase flow model, we must decide upon proper primary dependent variables after taking into account (1) computational efficiency; (2) robustness; and (3) simplicity in evaluating other secondary variables and setting up the linearized equations.

2. Flow-governing equations

Multiphase systems of interest in this study include the three cases: (1) one-active-phase water flow in unsaturated media, as described by Richards equation; (2) two-active-phase flow of water and gas (or air); and (3) three-active-phase flow of gas (air), water and NAPL. For simplicity, we focus on the formulation for three-phase flow and two-phase flow (of gas and water). One-active-phase flow can be considered a special case of three-phase flow.

The multiphase system in a porous or fractured formation is assumed to be composed of three phases: gas (air), water, and NAPL (oil). Although each of these three phases contains a number of components, they are treated here as a single "pseudo-component" with averaged properties of the fluids. In addition, the three fluid components of gas, water and NAPL are assumed to be present only in their associated phases. Each phase

flows in response to its pressure, gravitational, and capillary forces according to the multiphase extension of Darcy's law. In an isothermal system containing three mass components, three mass-balance equations are needed to fully describe the system for flow in a porous or fractured domain.

For flow of phase β (β = g for gas, β = w for water, and β = n for NAPL or oil):

$$\frac{\partial}{\partial t}\left(\phi S_\beta \rho_\beta\right) = -\nabla \cdot \left(\rho_\beta v_\beta\right) + q_\beta \tag{2-1}$$

where the Darcy velocity of phase β is defined by:

$$v_\beta = -\frac{k k_{r\beta}}{\mu_\beta}\left(\nabla P_\beta - \rho_\beta g \nabla D\right). \tag{2-2}$$

In Eqs. (2-1) and (2-2), ρ_β is the density of phase β under subsurface conditions; ϕ is the effective porosity of the formation; μ_β is the viscosity of phase β; S_β is the saturation of phase β; P_β is the pressure of phase β; q_β is the sink/source term of phase (component) β per unit volume of formation; g is gravitational acceleration; k is the absolute/intrinsic permeability (tensor) of the formation; $k_{r\beta}$ is relative permeability to phase β; and D is depth.

The governing Eq. (2-1) of mass balance for three-phase fluids needs to be supplemented with constitutive equations. The following relationships will be used to complete the description of multiphase flow through porous media.

For flow in a two-phase (one- or two-active-phase) system:

$$S_w + S_g = 1. \tag{2-3}$$

For three-phase flow:

$$S_w + S_n + S_g = 1. \tag{2-4}$$

The capillary pressures relate pressures between the phases. The aqueous and gas phase pressures are related by:

$$P_w = P_g - P_{cgw}\left(S_w\right) \tag{2-5}$$

where P_{cgw} is the gas–water capillary pressure in a gas–water, two-phase system or a three-phase (gas, water and NAPL) system; and it is assumed to be a function of water saturation only. The NAPL pressure is related to the gas phase pressure by:

$$P_n = P_g - P_{cgn}\left(S_w, S_n\right) \tag{2-6}$$

where P_{cgn} is the gas-NAPL capillary pressure in a three-phase system, which is a function of both water and NAPL saturations. For many aquifer formations, the wettability order is (1) aqueous phase, (2) NAPL phase, and (3) gas phase. The gas–water capillary pressure is usually stronger than the gas–NAPL capillary pressure. The NAPL–water capillary pressure, P_{cnw}, in a three-phase system, may be defined as:

$$P_{cnw} = P_{cgw} - P_{cgn} = P_n - P_w. \tag{2-7}$$

The relative permeabilities are assumed to be functions of fluid saturations only. The relative permeability to the water phase in a water–gas, two-phase or three-phase system is described by:

$$k_{\mathrm{rw}} = k_{\mathrm{rw}}(\mathrm{S_w}) \tag{2-8}$$

to the NAPL phase by:

$$k_{\mathrm{rn}} = k_{\mathrm{rn}}(S_{\mathrm{w}}, S_{\mathrm{g}}) \tag{2-9}$$

and to the gas phase by:

$$k_{\mathrm{rg}} = k_{\mathrm{rg}}(S_{\mathrm{g}}). \tag{2-10}$$

The densities of gas, water, and NAPL, as well as the viscosities of fluids under reservoir conditions, can in general be treated as functions of fluid pressures at a given temperaure.

3. Numerical formulation

3.1. Discrete equations

In this study, the flow formulation of Section 2 has been implemented into a general-purpose, two-phase flow simulator, the TOUGH2 code (Pruess, 1991), and a three-phase simulator MSFLOW code (Wu, 1998). One-phase, Richards' flow, is modeled using a modified version of the TOUGH2 EOS9 module (Wu et al., 1996a), which includes an option of selecting two types of primary variables for solving Richards' equation. The two active phase problem and the three-phase flow problems are handled using a special version of the MSFLOW code, which has the capability of selecting various sets of primary variables. As implemented in the TOUGH2 and MSFLOW codes, Eq. (2-1) can be discretized in space using an integral finite-difference or control-volume finite-element scheme for a porous and/or fractured medium. The time discretization is carried out with a backward, first-order finite-difference scheme. The discrete nonlinear equations for gas, water and NAPL at node i are as follows (for fully implicit time stepping):

$$\left\{\left(\phi S_\beta \rho_\beta\right)_i^{n+1} - \left(\phi S_\beta \rho_\beta\right)_i^{n}\right\}\frac{V_i}{\Delta t} = \sum_{j\in\eta_i}\left(\rho_\beta \lambda_\beta\right)_{ij+1/2}^{n+1}\gamma_{ij}\left[\psi_{\beta j}^{n+1} - \psi_{\beta i}^{n+1}\right] + Q_{\beta i}^{n+1}$$

$$\text{for } \beta(\beta = \mathrm{g}, \mathrm{w}, \text{and } \mathrm{n}) \tag{3-1}$$

where superscript n denotes the previous time level; $n+1$ is the current time level; V_i is the volume of element i (porous or fractured block); Δt is time step size; and η_j contains the set of neighbor nodes (j) (porous or fractured block) to which element i is

directly connected. Subscript $ij+1/2$ denotes an appropriate averaging of properties at the interface between two nodes i and j. The mobility of phase β is defined as:

$$\lambda_\beta = \frac{k_{r\beta}}{\mu_\beta}. \tag{3-2}$$

Mobilities are always upstream weighted in this study. The flow potential term in Eq. (3-1) is defined as:

$$\psi_{\beta i}^{n+1} = P_{\beta i}^{n+1} - \rho_{\beta, ij+1/2}^{n+1} g D_i \tag{3-3}$$

and the transmissivity γ_{ij} in Eq. (3-1) is defined, if the integral finite-difference scheme is used (Pruess, 1991), as:

$$\gamma_{ij} = \frac{A_{ij} k_{ij+1/2}}{d_i + d_j} \tag{3-4}$$

where A_{ij} is the common interface area between connected nodes i and j, d_i is the distance from the center of element i to the interface between nodes i and j, $k_{ij+1/2}$ is an averaged (e.g., harmonic weighted) absolute permeability along the connection between nodes i and j, and D_i is the depth to the center of node i. The mass sink/source term at element i, $Q_{\beta i}$ for phase β, is defined as:

$$Q_{\beta i}^{n+1} = q_{\beta i}^{n+1} V_i. \tag{3-5}$$

Discrete Eq. (3-1) applies in all the three scenarios studied in this work: (1) one-phase flow with only the water equation (β = w only) to be solved; (2) two-phase flow with water and gas equations (β = g and w) to be solved; and (3) three-phase flow with all three equations (β = g, w, and n) to be solved. The equation has the same form regardless of the dimensionality of the system (i.e., whether it is a one-dimensional, two-dimensional or three-dimensional flow domain).

3.2. Mass conservative discretization

A mass-balance check has been traditionally used to examine the accuracy and correctness of numerical solutions to subsurface flow problems. In petroleum reservoir simulation applications, mass conservative numerical schemes have been used exclusively (Coats, 1987) as well as in the geothermal studies (Pruess, 1987). In contrast, many of the "standard" numerical models, currently used in groundwater and soil science applications, have been based on nonmass-conservative methods for solving Richards' equation, as discussed in Cella et al. (1990). In recent years, the importance of using mass conservative numerical schemes has been recognized and implemented in the groundwater literature (e.g., Cella et al., 1990; Huyakorn et al., 1994; Forsyth et al., 1995; Berg, 1999). It should be pointed out that a nonmass-conservative numerical scheme may still give accurate and correct solutions with mass conservative results as long as both spatial and temporal discretization are sufficiently small. At the same time, at a mass conservative solution may not guarantee the accuracy of the solution, i.e.,

mass conservation is a necessary but not sufficient condition for convergence (Cella et al., 1990).

In this work, we are interested only in the mass-conservative formulation of the discretized equations. Note that the discrete Eq. (3-1) is exactly mass conservative for each phase fluid. This is because Eq. (3-1) states that the rate of change in mass accumulation of a phase at a node over a time step is exactly balanced by the inflow/outflow of the phase and sink/source terms on the right-hand side of the equation. Note that the transmissivity (Eq. (3-4)) has the property $\gamma_{ij} = \gamma_{ji}$, which indicates that flow from node i to node j is equal to and opposite to that from node j to node i. Therefore, no mass will be lost or created during the solution, and the discretization is mass conservative. A mass-conservative discretized equation such as Eq. (3-1) will guarantee a mass conservative solution to within the special convergence tolerance of the discrete algebraic equations.

There exists a significant inconsistency in the literature regarding the definition of a mass-conservative formulation, and in general there is confusion between mass-conservative discretized equations and mass-conservative discretization in the groundwater and soil-science literature. There have been various efforts, as discussed in Gee et al. (1991), to relate mass-balance errors with different formulations of the multiphase fluid flow governing equations and primary variable selection. This can only be explained as the consequence of using nonmass-conservative formulations or nonconverged solutions. Here, we define a mass-conservative scheme of a numerical formulation as a discretization that guarantees mass conservation for all phases, independent of how nonlinear equations are solved and which primary variables are selected. Once a converged solution is obtained, mass balance errors will become sufficiently small, which is related directly to the convergence tolerance specified for the problem.

3.3. Numerical solution scheme

In general, the discrete nonlinear Eq. (3-1) are solved using a Newton iteration scheme fully implicitly. Let us write Eq. (3-1) of mass balance in a residual form as:

$$R_i^{\beta,n+1} = \left\{ \left(\phi S_\beta \rho_\beta \right)_i^{n+1} - \left(\phi S_\beta \rho_\beta \right)_i^{n} \right\} \frac{V_i}{\Delta t} - \sum_{j \in \eta_i} \left(\rho_\beta \lambda_\beta \right)_{ij+1/2}^{n+1} \gamma_{ij} \left[\psi_{\beta j}^{n+1} - \psi_{\beta i}^{n+1} \right] - Q_{\beta i}^{n+1}$$

$$\text{for } \beta \ (\beta = \mathrm{g}, \mathrm{w} \text{ and } \mathrm{n};\ i = 1, 2, 3, \ldots, N) \tag{3-6}$$

where N is the total number of nodes of the grid. For a three-phase flow system, $3 \times N$ coupled nonlinear equations must be solved, with three equations at each node for the three mass-balance equations of gas, water, and NAPL, respectively. In general, three primary variables (x_1, x_2, x_3) are needed for each node. The primary variables are selected from fluid pressures and saturations in this work, and the rest of the dependent variables, such as relative permeability, capillary pressures, viscosity, and densities (as

well as nonselected pressures and saturations), are treated as secondary variables. The selection of primary variables is discussed below for the three flow scenarios. In terms of the primary variables, the Newton iteration scheme gives rise to:

$$\sum_m \frac{\partial R_i^{\beta,n+1}(x_{m,p})}{\partial x_m}\left(\delta x_{m,p+1}\right) = -R_i^{\beta,n+1}(x_{m,p}) \quad \text{for } m = 1, 2, \text{and } 3 \tag{3-7}$$

where index $m = 1$, 2, and 3 indicates the primary variable 1, 2, and 3, respectively, at node i and all its direct neighbors; p is the iteration level; and $i = 1, 2, 3, \ldots, N$. The primary variables are updated after each iteration:

$$x_{m,p+1} = x_{m,p} + \delta x_{m,p+1}. \tag{3-8}$$

A numerical method is used to construct the Jacobian matrix for Eq. (3-7). For a fully implicit element, the Jacobian is evaluated using numerical differentiation, as outlined by Forsyth et al. (1995). Eq. (3-7) represents a system of $3 \times N$ linearized equations for a three-phase flow problem, solved by an iterative sparse matrix solver (Forsyth, 1992). During a solution, the iteration is continued until the residuals $R_i^{\beta,n+1}$ for solving Richard's equation or changes in primary variables $\delta x_{m,p+1}$ over an iteration for two-phase and three-phase flow cases are reduced below a preset convergence tolerance.

3.4. Selection of primary variables

We have conducted a series of comparative studies to investigate the effects of different primary variables on numerical performance. Selections and comparisons of primary variables for the three scenarios of flow are discussed in this section. In certain cases, the primary variables are not static, and a dynamic variable substitution or switching may be needed, depending on the phase conditions of a node. In general, primary-variable selection and switching affects only the update of the secondary dependent variables and does not affect the equation setup, because the discrete equations [e.g., Eq. (3-6)] are still mass-conservation equations for each node regardless what primary or secondary variables are selected. With an efficient numerical scheme in evaluating the Jacobian matrix and residuals of Eq. (3-7), as discussed by Forsyth et al. (1995), primary variable selections and switching are straightforward to implement into a multiphase flow code.

3.4.1. Richards' equation

For one-active-phase flow, described by Richards' equation, only one equation of the linearized mass balance Eq. (3-7) per node needs to be solved. In this case, it has been shown (Forsyth et al., 1995) that a robust and efficient numerical approach is to use a water content- or saturation-based formulation with variable substitution, which works well under any flow conditions including heterogeneous systems with dry conditions. In this method, variable substitution is necessary for modeling flow in both unsaturated and saturated zones, because saturation is no longer a dependent variable under saturated flow conditions, and consequently the primary variable needs to be switched to a head- or pressure-based formulation for nodes that become fully saturated.

Theoretically, the pressure-based formulation works for both unsaturated and saturated conditions as well. However, this formulation is not robust and performs very poorly under dry flow conditions, when compared with the saturation-based formulation (Forsyth et al., 1995). Physically, a dry end corresponds to the steepest or infinite slope of a capillary curve, which makes a head or pressure formulation unstable with an infinitesimal change in water content. On the other hand, the mass-balance Eq. (3-6) is still very sensitive to changes in water saturation under the same dry conditions for a saturation-based formulation, because at least the accumulation of the equation is directly proportional to the saturation value. Water content or saturation is still well defined, which gives rise to a much better conditioned Jacobian (as seen in numerical experiments) and results in much smoother convergence.

We use the saturation-based formulation with variable substitution as a base-case in selecting primary variables, and use pressure-based formulation for comparison purpose. The two formulations and associated primary variables and variable-switching scheme are shown in Table 1 for studies of numerical simulations using Richards' equation.

3.4.2. Two-phase flow

Two mass balance equations need to be solved for two-phase flow of gas and water, with $\beta = g$ and w, in Eq. (3-7). We select two combinations of primary variables in this scenario, the first a mixed formulation of one pressure and one saturation, and the second a two-pressure formulation as shown in Table 2. It should be pointed out that the two-pressure formulation has found fewer applications in multiphase flow simulations in the literature, other than in some theoretical studies. This formulation suffers the same convergence problem as the pressure-based formulation for solving Richards' equation under dry conditions as discussed above. Furthermore, this method is unable to handle phase transitions on the wet end when the system becomes fully saturated (Binning and Celia, 1999). In general, the two-pressure formulation collapses at a single-phase condition where two pressures are no longer independent and at the same time two primary variables are still needed to solve two mass balance equations. In addition, the two-pressure formulation will break down for two-phase miscible displacement when the capillary pressure between the two phases becomes zero. In this study, we use the two-pressure formulation for comparison. In order to avoid collapse of the formulation, we use variable switching at both ends of the dry and wet conditions, i.e., switching to a mixed formulation when saturation is near the residual or unity.

Table 1
Choice and switching of primary variables for solving Richards' equation

Formulation	Phase	Primary variables
		x_1
Saturation-based with variable substitution	Two-phase	S_w
	Single-phase water	P_w
Pressure-based	Two-phase or single-phase water	P_w

Table 2
Choice and switching of primary variables for solving the two-phase flow equation

Formulation	Phase	Primary variables	
		x_1	x_2
Mixed	Two-phase, single-phase water, or single-phase gas	P_g	S_g
Two-pressure	Two-phase	P_g	P_w
	Single-phase water	P_w	S_g
	Single-phase gas	P_g	S_g

3.4.3. Three-phase flow

For three-phase flow, we select a mixed formulation only, i.e., one pressure and two saturations as primary unknowns. Dealing with phase appearance and disappearance is more important in modeling three-phase flow than in the case of two-phase flow, because most model domains may contain regions at a single or two phases only for a typical NAPL contamination site. Based on the discussion above, a three-pressure formulation is not appropriate. In this work, we focus on the selection of different mixed primary variables and comparing them with each other. Table 3 lists nine combinations of primary variables selected for three-phase modeling with the fully implicit method, each of which applies to phase conditions of one, two, or three existing fluids.

There is a special formulation that considers only two active liquid phases in a three-phase system in modeling NAPL flow in vadose zones (Faust, 1985). This model is similar to Richards' assumption in three-phase flow and it ignores gas-phase dynamics by assuming a constant gas-phase pressure. In this case, only two mass balance equations for water and NAPL need to be solved; therefore the formulation is more computationally efficient when applied. Forsyth et al. (1998) presented numerical experimental results for this formulation and concluded that use of two liquid saturations, associated with variable switching from water saturation to NAPL pressure to deal with the nodes of gas-phase disappearance provided the best numerical performance.

It should be pointed out that we scale the Jacobian by the inverse of one block diagonal before solving the matrix. Since pivoting is used to invert the block diagonal,

Table 3
Choice of primary variables for solving the three-phase flow equation

Formulation #	Primary variables		
	x_1	x_2	x_3
1	P_g	S_g	S_o
2	P_g	S_g	S_w
3	P_g	S_o	S_w
4	P_o	S_g	S_o
5	P_o	S_g	S_w
6	P_o	S_o	S_w
7	P_w	S_g	S_o
8	P_w	S_g	S_w
9	P_w	S_o	S_w

associations of different primary variables with mass-balance equations of the fluids for two- and three-phase flow formulations are immaterial in this study.

3.5. Fractured media

The technique for modeling flow through fractured rock follows the dual-continua methodology (Warren and Root, 1963; Pruess and Narasimhan, 1985; Wu and Pruess, 1988). This method treats fracture and rock–matrix flow, and interactions, using a multi-continua numerical approach, including the double- or multi-porosity method, the dual-permeability method, and the more general "multiple interacting continua" (MINC) method (Pruess and Narasimhan, 1985).

The model formulation in this work, as discussed above, is applicable to both single-continuum and multi-continua media. This fracture–matrix mesh is usually based on a primary, single-porous medium mesh, which is generated using only geometric information. Within a certain reservoir subdomain (corresponding to one finite-difference gridblock of the primary mesh), all fractures will be lumped into a fractured continuum. All matrix material within a certain distance from the fractures will be lumped into one or several different matrix continua, as required by the double-porosity, dual-permeability, or MINC approximations. Several matrix subgridding schemes exist for designing different meshes with different fracture–matrix conceptual models (Pruess, 1983).

Once a proper mesh for the fracture–matrix system is generated, fracture and matrix blocks are specified to represent fracture or matrix domains, separately. Formally, they are treated exactly the same during the solution in the model. However, physically consistent fracture and matrix properties, weighting schemes and modeling conditions must be appropriately specified for fracture and matrix systems, respectively.

3.6. Initial and boundary conditions

The initial status of a multiphase system needs to be specified by initially assigning a complete set of primary variables to each gridblock. A commonly used procedure for specifying a capillary–gravity equilibrium condition is the restart option, in which a complete set of initial conditions is produced in a previous simulation with appropriate boundary conditions.

First-type or Dirichlet boundary conditions denote constant- or time-dependent phase pressure and saturation conditions. These types of boundary conditions can be treated using the large-volume method, in which a constant pressure/saturation node is specified with a numerically large volume while keeping all the other geometric properties of the mesh unchanged. However, caution should be taken to (1) identify phase conditions when specifying the "initial condition" for the large-volume boundary node and (2) distinguish upstream/injection from downstream/production nodes. Once specified, primary variables will be fixed at the large-volume boundary nodes, and the code handles these boundary nodes exactly like any other computational nodes.

Flux-type or Neuman boundary conditions are treated as constant or time-dependent sink/source terms, depending on the pumping (production) or injection condition, which

can be directly added to Eq. (3-6). They are all implemented fully implicitly. This treatment of flux-type boundary conditions is especially useful for a situation where flux distribution along the boundary is known, such as dealing with surface infiltration. This method may also be used for an injection or pumping well connected to a single gridblock without injection or pumping pressures to be estimated. More general treatment of multilayered well boundary conditions is discussed in Wu (1999, 2000).

4. Test problems

We present three test examples in this section to investigate computational performance when selecting different primary variables in numerical formulations for one active phase, two-phase and three-phase flow problems, respectively, including:

1. three-dimensional liquid flow in unsaturated fractured rock using Richards' equation for comparisons of saturation-based and pressure-based formulations
2. two-dimensional gas–water, two-phase flow in unsaturated fractured rock for comparisons of mixed and two-pressure formulations
3. three-dimensional gas–water–oil, three-phase flow with air injection in an unconfined aquifer for comparisons of different primary variable selections.

4.1. Test 1—three-dimensional liquid flow in unsaturated fractured rocks

The first example is based on a large mountain scale model developed for investigations of the unsaturated zone (UZ) at Yucca Mountain, NV (Wu et al., 1998, 1999). The unsaturated zone of Yucca Mountain has been selected as a potential subsurface repository for storage of high-level radioactive wastes of the U.S. Since the mid-1980s, the U.S. Department of Energy has pursued a program of site-characterization studies designed to explore the geological, hydrological, and geothermal conditions in the unsaturated and saturated zones of the mountain.

The thickness of the unsaturated zone at Yucca Mountain varies between about 500 and 700 m, depending on local topography. The potential repository would be located in the highly fractured Topopah Spring welded unit (TSw), about 300 m above the water table and 300 m below the ground surface. Subsurface flow and transport processes at Yucca Mountain occur in a heterogeneous environment of layered, anisotropic, fractured volcanic rocks (Scott and Bonk, 1984; Rousseau et al., 1996). These volcanics consist of alternating layers of welded and nonwelded ash flow and air-fall tuffs, with welded tuffs generally having much lower matrix permeability but considerably higher fracture permeability than the nonwelded tuffs. These geologic formations are organized into hydrogeologic units roughly based on the degree of welding (Montazer and Wilson, 1984): (from the land surface downwards) the Tiva Canyon welded (TCw), the Paintbrush nonwelded unit (PTn), the Topopah Spring welded (TSw) unit, the Calico Hills nonwelded (CHn), and the Crater Flat undifferentiated (CFu) units. In addition to the highly heterogeneous and anisotropic nature of the fractured tuffs existing at the

mountain, flow and transport processes are complicated by numerous strike-slip and normal faults with varying amounts of offset. The complexity in the hydrogeological settings and high contrast in fracture and matrix properties result in a challenging numerical simulation problem (Wu et al., 1999).

The 3-D model domain and the numerical grid for this study are shown in a plan view in Fig. 1. The model domain covers a total area of approximately 43 km^2, roughly from 2 km north of borehole G-2 in the north to borehole G-3 in the south, and from the Bow Ridge fault in the east to about 1 km west of the Solitario Canyon fault. Fig. 1 indicates the numerical grid with increased resolution in the vicinity of the proposed

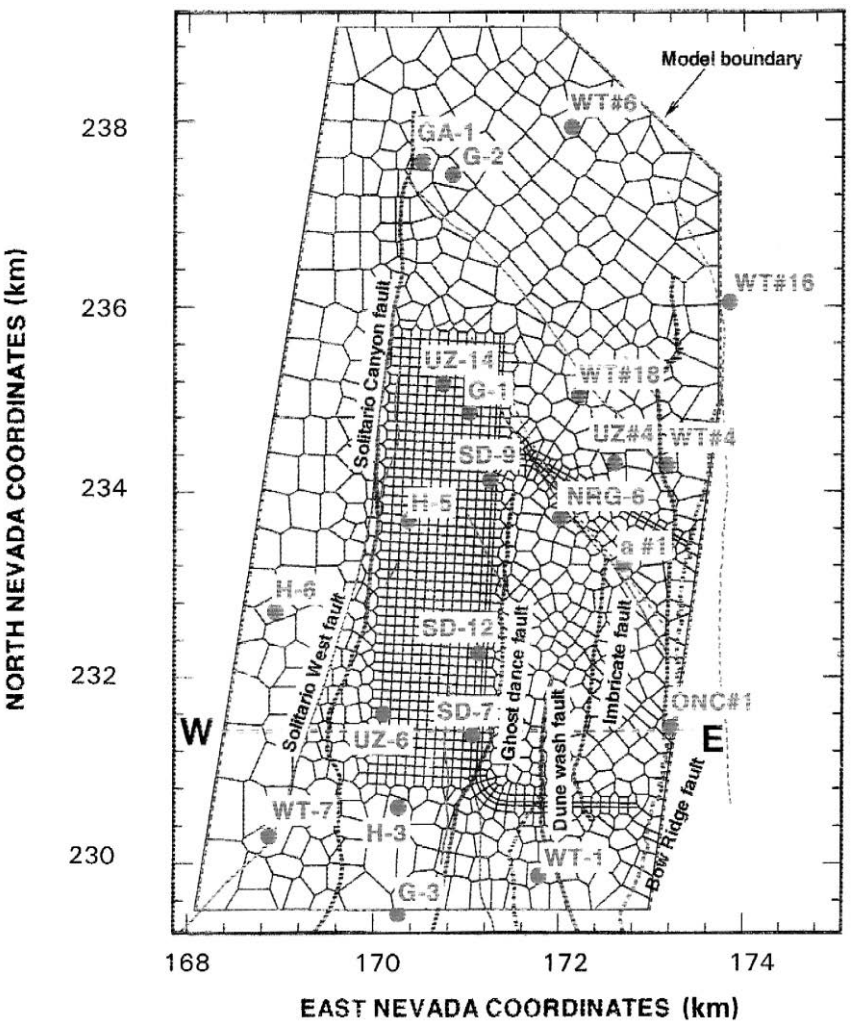

Fig. 1. Plan view of the three-dimensional site-scale model domain, grid and incorporated major faults.

repository, located near the center of the model domain. Also shown in the figure are the locations of a number of boreholes used for model calibration and references. As shown in Fig. 1, several major faults are incorporated explicitly in the model, including the Solitario Canyon, Ghost Dance, Dune Wash, and Bow Ridge faults. Some of these faults are not labeled on the figure. The Bow Ridge fault is treated as the eastern boundary of the model domain. Based on field evidence indicating that the fault zones are predominantly vertical or near vertical at Yucca Mountain, the faults are represented in the model as vertical zones of finite thickness bounded by sudden stratigraphic offsets in connection to adjacent gridlayers. The scheme used for generating the fault grid elements was outlined by Wittwer et al. (1995).

In the vertical direction, the layering and subdivision of geological units in the numerical grid are based on the geological model of Bandurraga (1996). Fig. 2 shows the hydrogeological layers and offsets of the explicitly modeled faults in west–east vertical cross-section along line WE of Fig. 1. The 3-D model grid has 28 computational grid layers that represent the different hydrogeological units and layers in the unsaturated zone of the Mountain. A dual-continua (i.e., dual-permeability approach) is used here to handle fracture–matrix flow and interactions.

Each model layer of the grid (Fig. 1) has 1470 irregular gridblocks for a total of about 40,000 gridblocks. The 3-D grid was generated employing a Voronoi-type mesh (Palagi and Aziz, 1994). A dual-permeability grid was generated based on the primary grid (Fig. 1). The dual-permeability mesh subdivides each primary mesh element into fracture and matrix domains, resulting in a grid of 80,000 gridblocks and 310,000 connections.

The boundary conditions are specified as follows. The ground surface is taken as the top model boundary, and the water table is regarded as the bottom boundary. The bottom boundary of the model are treated as Dirichlet-type boundaries, i.e., constant (but spatially distributed) pressures and constant liquid saturations are specified along these boundary surfaces. On the top boundary, a spatially varying, steady-state infiltration map (Flint et al., 1996) is used in this study to describe the net steady-state water recharge, with an average infiltration rate of 4.9 mm/year over the model domain. In addition, all the lateral boundaries surrounding the model domain (Fig. 1) are considered as closed boundaries.

Initially, uniform water saturation of 0.5 was specified to all grid blocks of fractures and matrix, except for the bottom boundary nodes, as initial conditions for the S-based simulation. For pressure–based formulation run, 0.5 water saturation was converted into pressures as initial conditions, i.e., the same physical conditions to start with.

In this study, an isothermal condition is assumed with constant temperature of 25°C. The properties used for fluids, rock matrix, and fractures, including two-phase flow parameters of fractures and matrix characteristics, were estimated based on field tests and model calibration studies, as summarized in Wu et al. (1998).

Two simulations were conducted for this problem, one using saturation-based (S-based) formulation with variable substitution for saturated nodes and one using pressure-based (P-based) formulation (Table 1). In the two simulations, the same convergence tolerance and time-stepping scheme were specified for a fair comparison. The simulations were both run to 2700 years of simulation time. Simulation results are

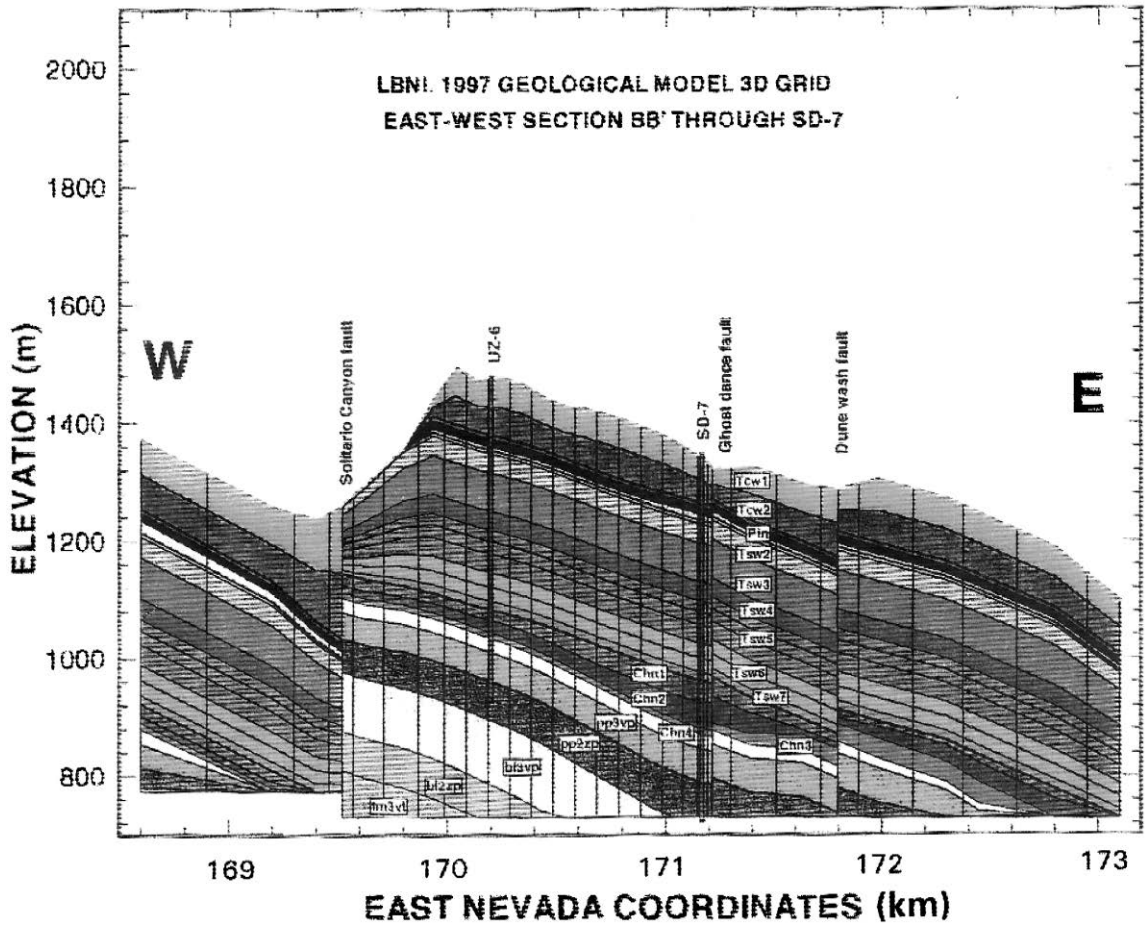

Fig. 2. West–east vertical cross-section through the 3-D model showing hydrogeological layers and offsets on the explicitly modeled faults.

shown in part in Figs. 3–5 for matrix liquid saturations in boreholes SD-7, SD-9 and SD-12 (see Fig. 1 for the borehole locations). Note that the current moisture conditions, as shown in Figs. 3–5 (labeled as "USGS Data"), in the unsaturated zone of Yucca Mountain are commonly conceptualized as those corresponding to the steady-state ambient conditions. Here we use the simulation results of 2700 years to approximate a steady-state condition by comparing them with the observations. Figs. 3, 4 and 5 indicate that the two formulations give almost identical results for the modeled liquid saturations in rock matrix, and the numerical results are in reasonable agreement with the field observations ("USGS data"), used in Wu et al. (1998), in all the cases. We have checked comparisons with many others boreholes, and the comparisons are similar to the results, as shown in Figs. 3–5.

Table 4 presents computational statistics for the numerical performances of the two formulations. The heading "inner iterations" denotes total numbers of iterations inside

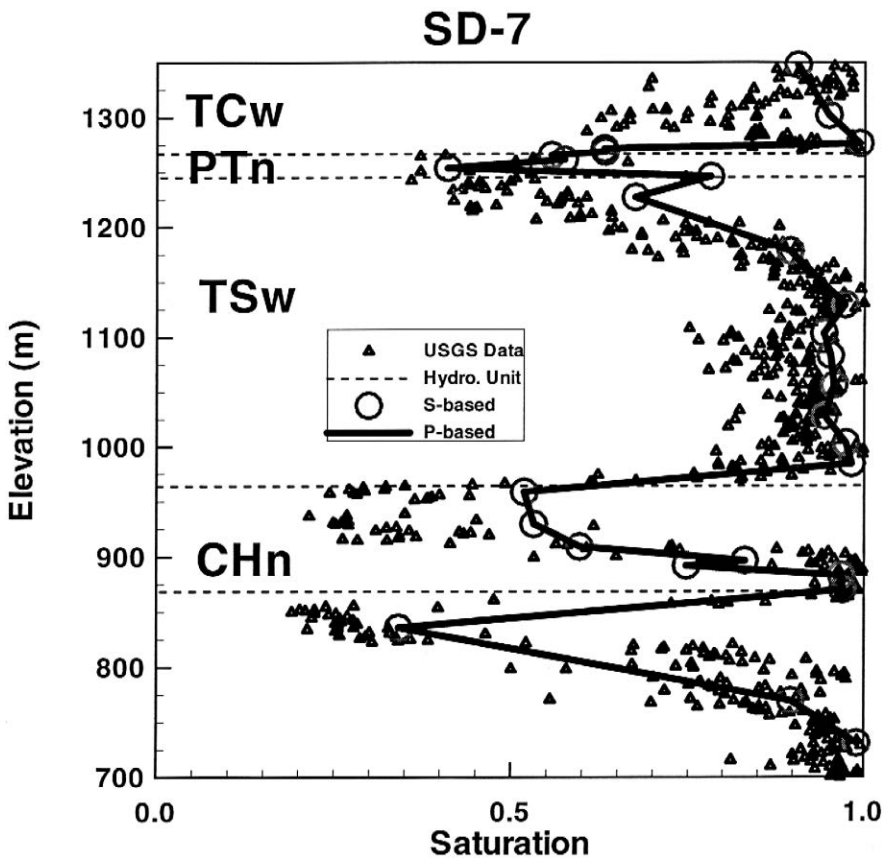

Fig. 3. Comparisons of matrix liquid saturations, simulated using the two formulations, and field observation data for borehole SD-7.

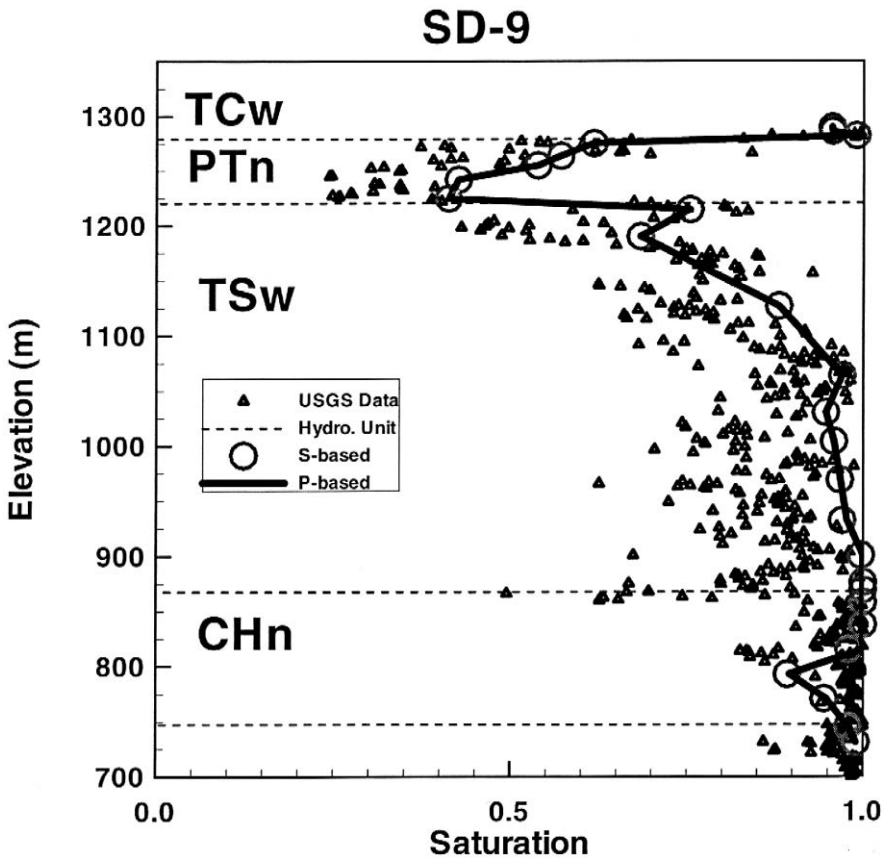

Fig. 4. Comparisons of matrix liquid saturations, simulated using the two formulations, and field observation data for borehole SD-9.

the linear-equation solver, and the CPU times were recorded on a DEC-alpha workstation. Of course, if identical time steps are used and the algebraic equations are solved to similar accuracy, then the computed solutions should be the same regardless of the choice of primary variables. The small differences in solutions result from the fact that even though the same convergence tolerances were used for both choices of primary variables, the actual solution accuracy for each method is slightly different (i.e., the final residuals that meet the convergence tolerance criteria are not identical). The simulation results of the two runs are very similar, as given in Figs. 3, 4 and 5; however, Table 4 shows that the S-based, mixed formulation performs 22 times faster than the P-based formulation for this particular problem of unsaturated flow in highly heterogeneous fractured rocks. During the test, we have also observed that the S-based, mixed formulation is not only more efficient, but also much more robust than the P-based method. The S-based method with variable substitution works for any initial and boundary conditions.

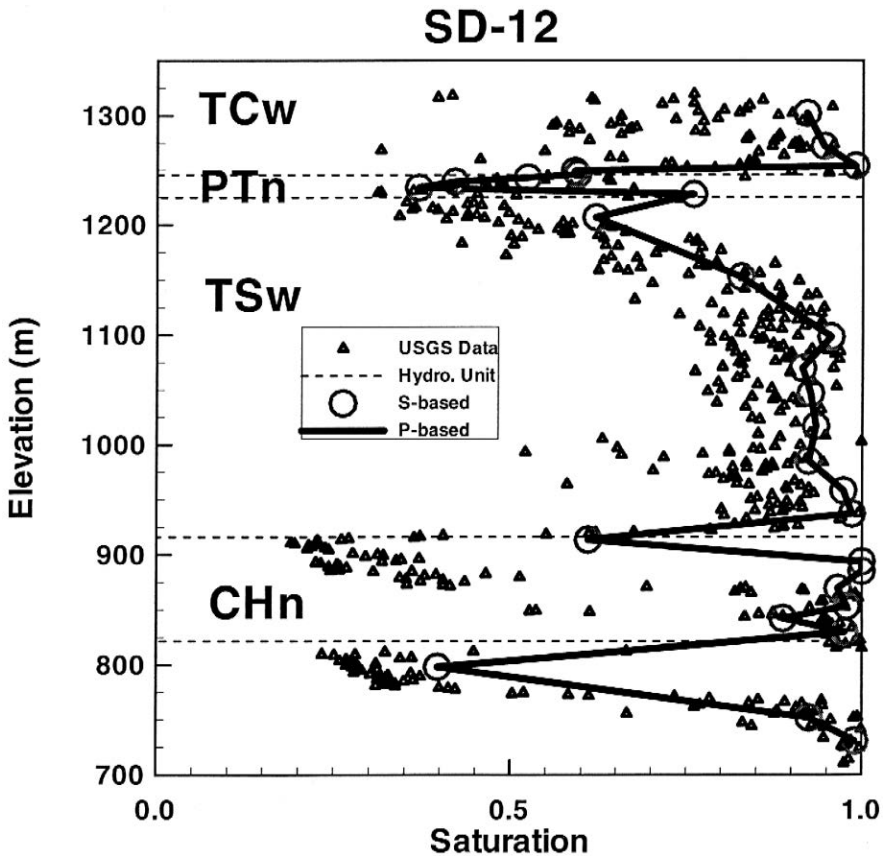

Fig. 5. Comparisons of matrix liquid saturations, simulated using the two formulations, and field observation data for borehole SD-12.

4.2. Test 2—two-dimensional, two-phase flow in unsaturated fractured rock

The second example is for comparison of two-active-phase, gas–water flow using two formulations (Table 2): one saturation and one pressure (mixed), and two pressures as primary variables. A two-dimensional west–east, vertical cross-section model is selected, along the middle of the repository near Borehole UZ-14 (Fig. 1), as shown in

Table 4
Comparison of numerical results for Test 1—three-dimensional flow in unsaturated rocks

Method	Time steps	Newton iterations	Inner iterations	CPU times (min)	Normalized CPU times
Saturation-based/mixed	364	1474	3980	196	1
Pressure-based	9000	40,245	49,100	4454	22.7

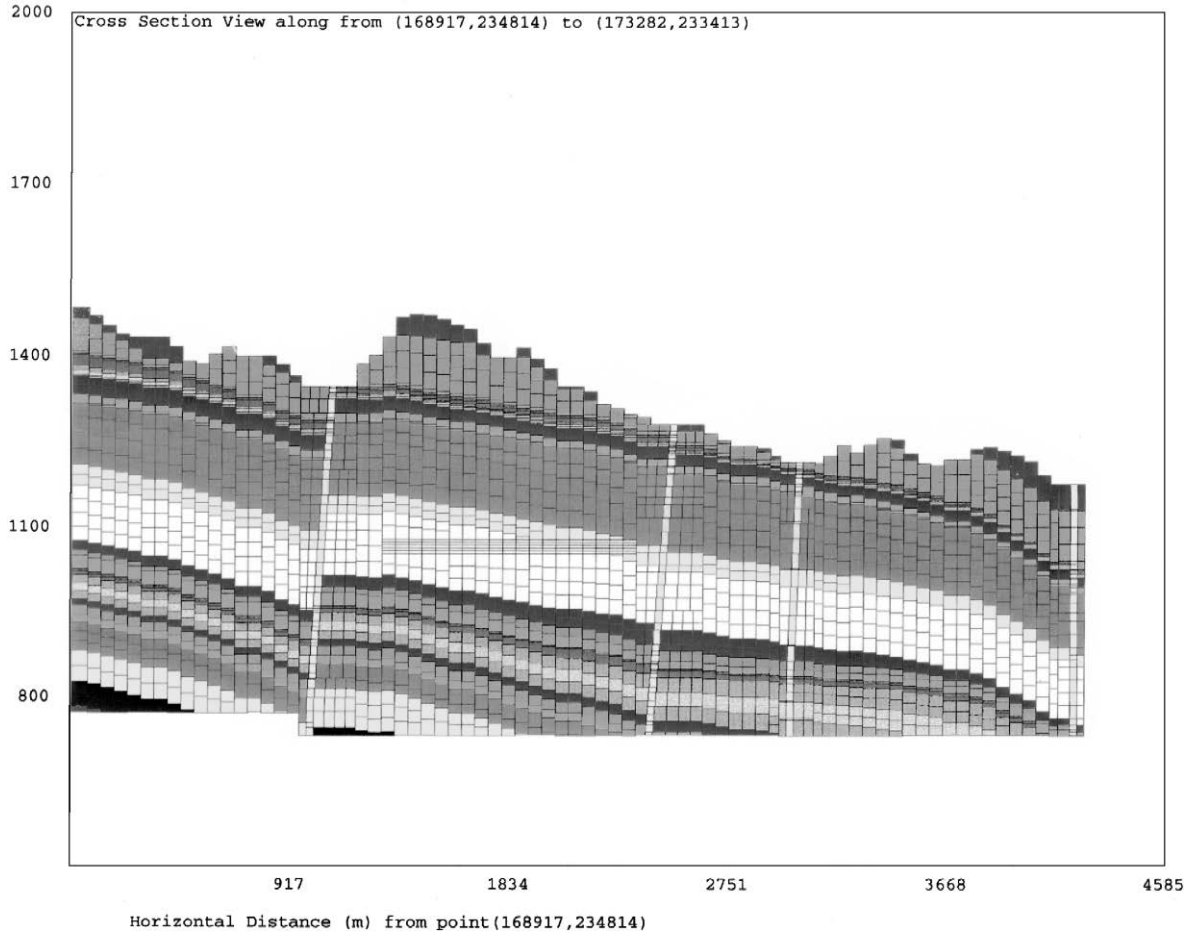

Fig. 6. Two-dimensional, west–east, cross-section grid, showing the vertical layering, faults and repository location.

Fig. 6 for the entire 2-D model domain and grid. Again, a dual-permeability approach is used for fracture–matrix interactions in this study. The irregular vertical grid, which includes four inclined faults, is designed for this two-dimensional cross-section, as displayed in Fig. 6. The grid is locally refined at the repository horizon by three 5-m-thick layers and the actual repository length along the middle section. The grid has a horizontal spacing of 56 m and vertical spacing of no more than 30 m. The 2-D model has approximately 6300 fracture and matrix elements, and 16,000 connections.

The boundary conditions are similar to those used by the 3-D model of Test 1. The ground surface is taken as the top model boundary. The water table is taken as the bottom boundary, with fixed liquid saturation and gas pressure specified. The surface infiltration map is implemented as source terms to the fracture gridblocks in the upper boundary and the resulting infiltration rates varying along each gridblock, with an average of 1.9 mm/year along the cross-section. An isothermal condition of 25°C is assumed for the system. Fluid and rock properties for this problem are taken from those for the recent modeling studies at Yucca Mountain (Bodvarsson et al., 1998).

To make a fair comparison of the two formulations of Table 2 (Table 1) for the two-phase flow problem, we specified the same convergence tolerance with $\delta P = 1000$ Pa and $\delta S = 0.01$, and time-stepping scheme. In this problem, an automatic time-stepping option was invoked with using a constant time-step increasing multiplier (1.5) and a cutting factor (0.5). However, we found that the two-pressure formulation was not robust and could not handle a uniform initial condition. Therefore, the actual initial condition, specified for the two simulations, was generated using the results of mixed formulation, which correspond to the flow condition after 100 years surface infiltration with a uniform saturation guess initially.

The two simulations were both run to 100,000 years of simulation time, at which time the system has almost reached a steady state. Figs. 7 and 8 display contours of liquid saturations of matrix and fracture, respectively, along the cross-section. On the top of the figures is shown the nonuniformly distributed surface infiltration map. Figs. 7 and 8 show that in this case the two formulations predict nearly identical results for both matrix and fracture saturations.

Computational statistics for the numerical solution of the two formulations are given in Table 5 (simulations were conducted on a DEC-alpha workstation). Table 5 shows that the two formulations perform almost the same numerically in terms of both iterations and CPU times for this test problem. This is because (1) no phase transition occurs in the system with two phases present all the time and (2) good, smooth initial conditions exist to start with—the ideal conditions for the two-pressure formulation. However, the two-pressure formulation cannot be used for an arbitrary initial condition, and its performance is still no better than the mixed formulation.

4.3. Test 3—three-dimensional, three-phase flow of air, water and NAPL

The problem was adopted from an air injection study (Wu et al., 1996b), and it concerns three-phase well flow in a three-dimensional, layered system, consisting of a quarter of a five-spot well pattern, with constant-rate air injection and pumping wells, located diagonally, as shown in Fig. 9. The computational domain is 100 m (x) × 100 m

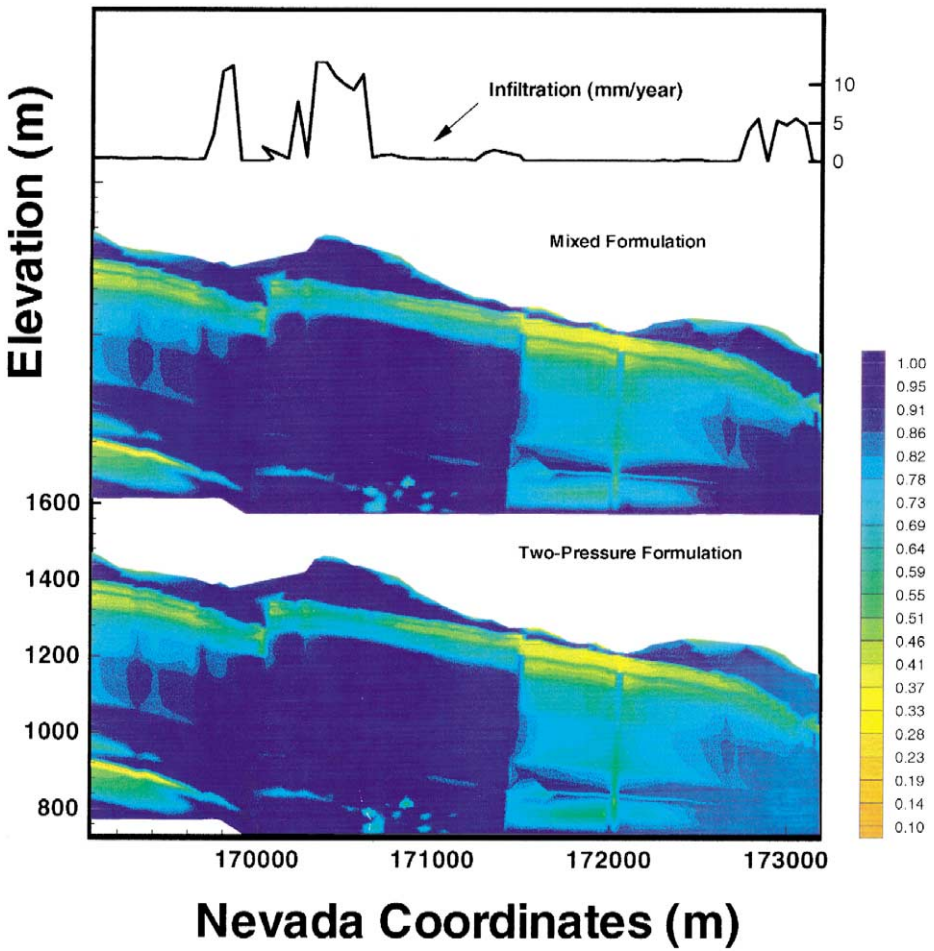

Fig. 7. Comparisons of matrix liquid saturations, simulated using the two formulations, along the west–east cross-section.

$(y) \times 10$ m (z), and is discretized using a $10 \times 10 \times 20$ grid. Node spacing in the x and y direction is a constant 10 m, while in the z (vertical) direction, the spacing is 0.5 m.

Air is injected at 1000 m^3/day (constant rate at standard conditions) with the injection well located at $x = 100$ m, $y = 100$ m and 3.5 m $< z <$ 5.5 m. The pumping well is located at $x = y = 0$ m, and 3.5 m $< z <$ 5.5 m and subject to a constant liquid (water + NAPL) rate of 10 m^3/day. The wells are both screened over a 2-m length.

As shown in Fig. 9, the modeled unconfined aquifer consists of four horizontal layers with different rock properties. A horizontal water table is approximately at an elevation of $z = 5$ m. In addition to the air-injection and liquid-pumping rates, the atmospheric condition and bottom water pressure are also described to enforce constant air pressure at the top boundary as well as stable water table conditions at the bottom. The initial

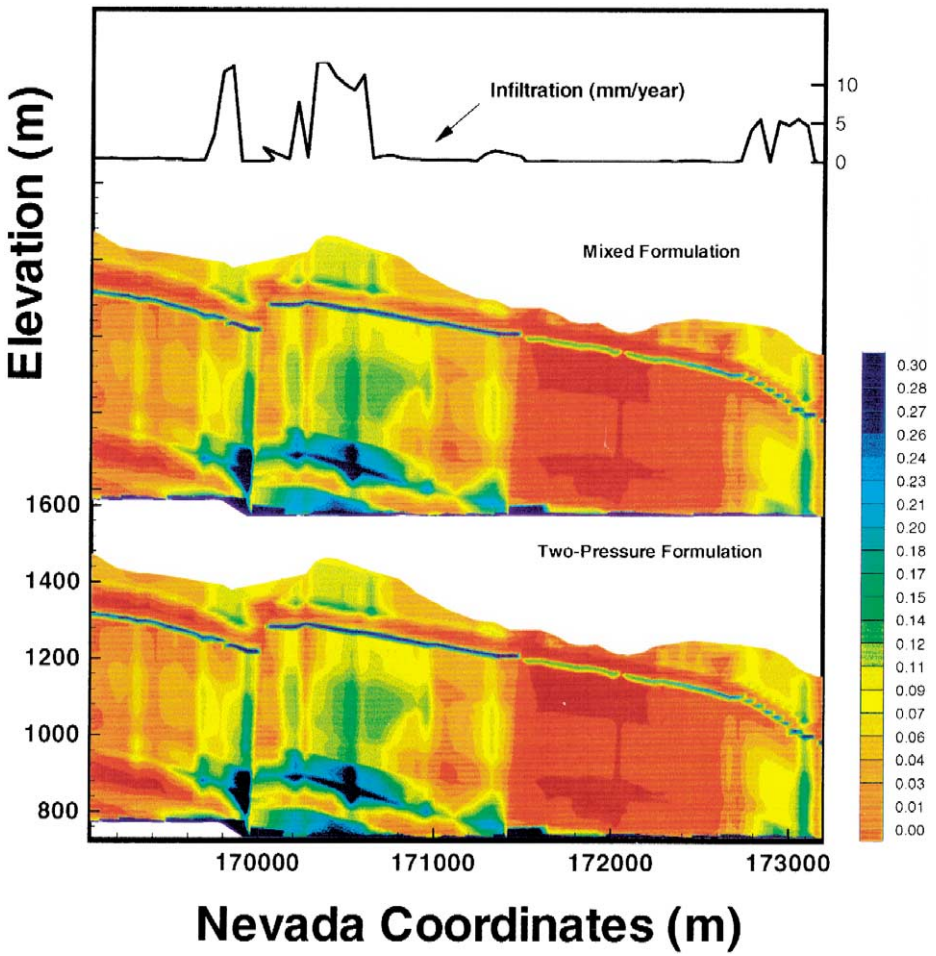

Fig. 8. Comparisons of fracture liquid saturations, simulated using the two formulations, along the west–east cross-section.

condition of the system is generated by placing a NAPL layer of 2.5 m in height along the water table and letting the system equilibrate. Fig. 10 illustrates the initial vertical profiles of water and NAPL saturations in the model domain. After the system is

Table 5
Comparison of numerical results for Test 2—two-dimensional, two-phase flow in unsaturated rocks

Method	Time steps	Newton iterations	Inner iterations	CPU times (s)	Normalized CPU times
Saturation-based/mixed	3213	3412	7244	2191	1
Two-pressure	3263	3414	7169	2199	1.004

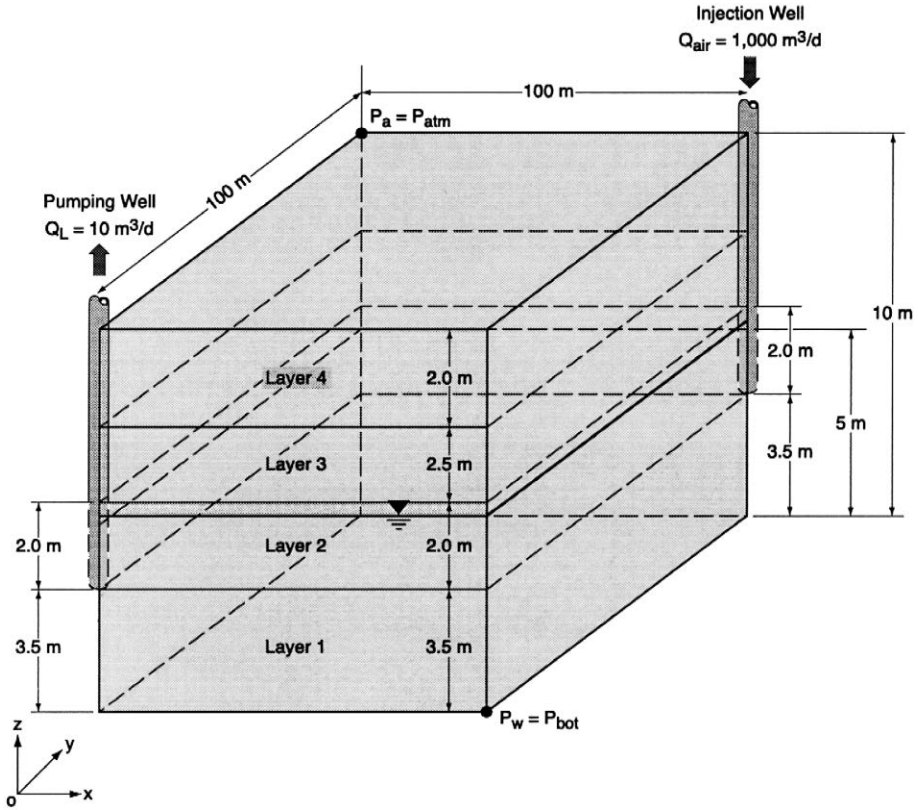

Fig. 9. Domain of air-injection problem.

equilibrated, air injection and liquid production are carried out for 100 days. Again, we specified the same convergence tolerance with $\delta P = 100$ Pa and $\delta S = 0.001$ for all the runs in this problem, and the time-stepping parameters were the same as those used in Test 2.

The input data of fluid properties, including relative permeability and capillary pressure curves for the layers, are given by Wu et al. (1996b). Scaled van Genuchten functions (Parker et al., 1987) are used here for evaluating the three-phase relative permeabilities and capillary pressures. We use this problem to test all the formulations of Table 3 for three-phase flow simulations. The simulations were all run to 100 days since liquid pumping and air injection start. Altogether nine different formulations (Table 3) were tested in this three-phase NAPL problem, including all the combinations of one pressure and two-saturation, mixed formulations (Table 3).

The simulated cumulative NAPL recovery rate from the pumping well at 100 days is about 7% of the total initial NAPL in the system. Examination of the simulation results for all the nine cases indicate that all the methods result in essentially the same NAPL recovery rates after 100 days air injection and pumping. Table 6 lists the statistics for numerical performances of each formulation in solving the problem (simulations were

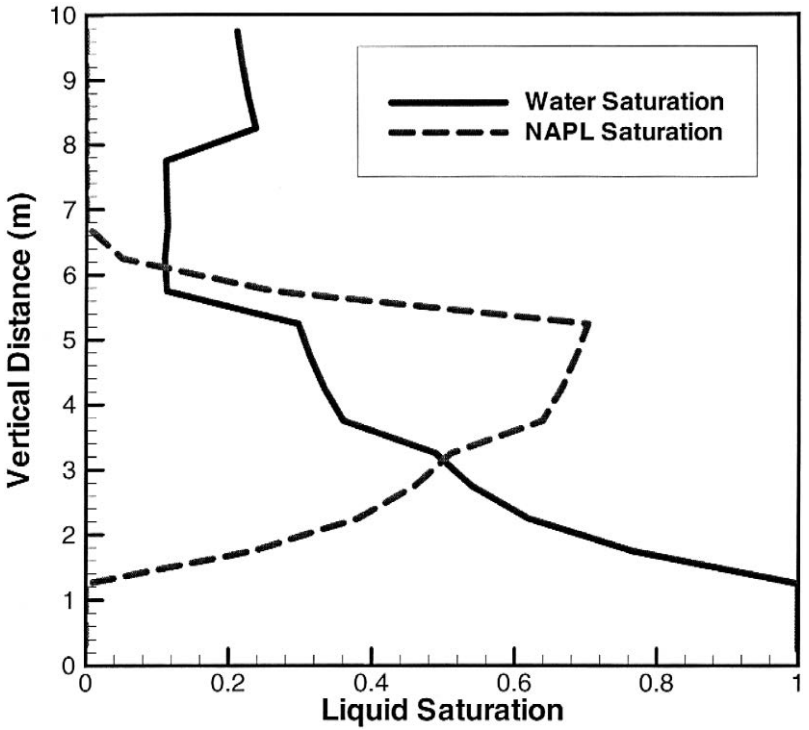

Fig. 10. Initial vertical profiles of water and NAPL saturations for the air-injection problem.

conducted on a Pentium II PC). Note that Table 6 indicates that performances of formulations with different pressure and saturation combinations are very different from each other for this test problem. Overall, the formulations using gas pressure (P_g) as a primary pressure variable perform the best in terms of CPU times required. In addition,

Table 6
Comparison of numerical results for Test 3—three-dimensional, three-phase flow of air injection in an unconfined aquifer

Primary variables	Time steps	Newton iterations	CPU times (s)	Normalized CPU times
$P_g - S_g - S_o$	346	1561	4238	1.16
$P_g - S_g - S_w$	173	1650	4696	1.24
$P_g - S_o - S_w$	312	1454	3798	1.00
$P_o - S_g - S_o$	825	6398	16,109	4.24
$P_o - S_g - S_w$	841	5599	14,389	3.79
$P_o - S_o - S_w$	1324	10,147	25,065	6.60
$P_w - S_g - S_o$	1124	7500	19,006	5.00
$P_w - S_g - S_w$	1527	9713	23,183	6.10
$P_w - S_o - S_w$	856	5256	12,816	3.37

we found during the testing that selecting P_g as a primary pressure variable was more robust than using P_w or P_o for this problem.

In general, in addition to the primary variables selected the numerical performance of multiphase flow models depends also on relative permeability and capillary functions, hydrogeological conditions and heterogeneity of aquifers, and the imposed boundary operational conditions imposed. The results of Table 6 and our past experiences indicate that using a gas-phase pressure with two saturations often performs better for simulating NAPL flow through unconfined aquifer systems and at the same time, selection of saturations is not very critical. This may be because in many cases, gas pressure is well defined and controlled by the surface atmospheric condition and stays relatively stable during a simulation. On the other hand, water or NAPL pressure will vary rapidly as infiltration or recharge conditions change with gas pressure held nearly constant, which may keep the solutions from converging.

5. Summary and conclusions

In this work, we present a comparative analysis of the selection (and subsequent effect) of primary variables in solutions for the discrete equations of multiphase flow simulations. The discussion of simulation results is based on a general, mass-conservative, discretized formulation for modeling multiphase, multi-dimensional flow through porous and fractured rocks. We have performed a series of numerical tests using large-scale field-simulation examples, including modeling one-active-phase, two-phase, and three-phase flow problems in multi-dimensional, heterogeneous fractured and porous rocks.

This study indicates that proper primary variable selection is crucial for efficiently solving a highly nonlinear multiphase subsurface flow problem using a Newton iteration. The selection of primary variables depends in general on how sensitive the system of equations is to the variables selected at given phase and flow conditions, leading to a better-conditioned Jacobian matrix. When determining primary variable selections in formulating a multiphase flow problem, we must take into account (1) computational efficiency, (2) robustness, and (3) simplicity in evaluating other secondary variables and setting up linearized equations.

The standard, head- or pressure-based formulation is found to perform very poorly numerically in solving Richards' equation for flow through highly heterogeneous fractured rocks. On the other hand, use of pressures only as primary variables in a two-active-phase or three-phase flow formulation creates difficulties in handling single-phase conditions or phase transition without implementing a variable substitution scheme. Numerically, the pressure-only method offers no advantages over a mixed formulation in terms of efficiency or sophistication of coding, and therefore in practice has little to offer. Based on this work and our previous experience, the following recommendations are suggested for selecting primary variables in multiphase flow formulation:

- saturation-based formulation with variable switching should be used for solving Richards' equation of one active phase liquid flow.

- one pressure (preferably gas pressure for unconfined aquifers) and one saturation (mixed) formulation should be used for two-active-phase flow.
- one pressure (preferably gas pressure for unconfined aquifers) and two-saturation (mixed) formulation should be used for three-phase flow.

Acknowledgements

The author is grateful to Jianchun Liu for reviewing this paper. This work was in part supported by the Assistant Secretary for Energy Efficiency and Renewable Energy, Office of Geothermal and Wind Technologies of the U.S. Department of Energy, under Contract No. DE-AC03-76SF00098.

References

Abriola, L.M., Pinder, G.F., 1985. A multiphase approach to the modeling of porous media contamination by organic compounds: 1. Equation development. Water Resources Research 21 (1), 11–18.

Aziz, K., Settari, A., 1979. Petroleum Reservoir Simulation. Applied Science Publishers, London.

Bandurraga, T.M., 1996. Geological Model Development and Vertical Layering Scheme for the Numerical Grid, Chapter 2 of "Development and Calibration of the Three-Dimensional Site-Scale Unsaturated-Zone Model of Yucca Mountain, Nevada." Edited by G. S. Bodvarsson and M. Bandurraga, Yucca Mountain Site Characterization Project Report, Lawrence Berkeley National Laboratory, Berkeley, CA.

Berg, P., 1999. Long-term simulation of water movement in soils using mass-conserving procedures. Advances in Water Resources 22 (5), 461–478.

Binning, P., Celia, M.A., 1999. Practical implementation of the fractional flow approach to multi-phase flow simulation. Advances in Water Resources 22 (5), 419–430.

Bodvarsson, G.S., Sonnenthal, E., Wu, Y.S., Eds., 1998. Unsaturated Zone Flow and Transport Modeling of Yucca Mountain, Nevada—Fiscal Year 1998 Report, Yucca Mountain Site Characterization Project Report, Milestone SP3CKJM4, Lawrence Berkeley National Laboratory, Berkeley, CA.

Cella, M.A., Bouloutas, E.T., Zarba, R.L., 1990. A general mass-conservative numerical solution for the unsaturated flow equations. Water Resources Research 26 (7), 1483–1496.

Coats, K.H., 1987. Reservoir Simulation, Chap. 48. Petroleum Engineering Handbook. Society of Petroleum Engineers, Richardson, TX, pp. 48-1–48-20.

Coats, K.H., Nielsen, R.L., Terhune, M.H., Weber, A.G., 1967. Simulation of three-dimensional, two-phase flow in oil and gas reservoirs. AIME Transactions 240, 377–388.

Cooley, R.L., 1983. Some new procedures for numerical solution of variably saturated flow problems. Water Resources Research 19 (5), 1271–1285.

Douglas Jr., J., Peaceman, D.W., Rachford Jr., H.H., 1959. A method for calculating multi-dimensional immiscible displacement. AIME Transactions 216, 297–306.

Falta, W.R., Pruess, K., Javandel, I., Witherspoon, P.A., 1992a. Numerical modeling of steam injection for the removal of nonaqueous phase liquids from the subsurface: 1. Numerical formulation. Water Resources Research 28 (2), 433–449.

Falta, W.R., Pruess, K., Javandel, I., Witherspoon, P.A., 1992b. Numerical modeling of steam injection for the removal of nonaqueous phase liquids from the subsurface: 2. Code validation and application. Water Resources Research 28 (2), 451–465.

Faust, C.R., 1985. Transport of immiscible fluids within and below the unsaturated zone: a numerical model. Water Resources Research 21 (4), 587–596.

Flint, A.L., Hevesi, J.A., Flint, E.L., 1996. Conceptual and Numerical Model of infiltration for the Yucca Mountain Area, Nevada, U.S. Geological Survey, Water-Resources Investigation Report, Denver, CO.

Forsyth, P.A., 1988. Simulation of nonaqueous phase groundwater contamination. Advances in Water Resources 11 (2), 74–83.

Forsyth, P.A., 1991. A control volume finite element approach to NAPL groundwater contamination. SIAM J. Sci. Statist. Comput. 12 (5), 1029–1057.

Forsyth, P.A., 1992. MATB User's Guide, Iterative Sparse Matrix Solvers for Block Matrices, University of Waterloo, Waterloo, Ontario, Canada.

Forsyth, P.A., 1994. Three-dimensional modeling of steam flush for DNAPL site remediation. International Journal for Numerical Methods in Fluids 19, 1055–1081.

Forsyth, P.A., Shao, B.Y., 1991. Numerical simulation of gas venting for NAPL site remediation. Advances in Water Resources 14 (6), 354–367.

Forsyth, P.A., Wu, Y.S., Pruess, K., 1995. Robust numerical methods for saturated–unsaturated flow with dry initial conditions in heterogeneous media. Advances in Water Resources 18, 25–38.

Forsyth, P.A., Unger, A.J.A., Sudicky, E.A., 1998. Nonlinear iteration methods for nonequilibrium multiphase subsurface flow. Advances in Water Resources 21, 433–499.

Gee, G.W., Kincaid, C.T., Lenhard, R.J., Simmons, C.S., 1991. Recent studies of flow and transport in the vadose zone. Contributions in Hydrology, U.S. National Reports to International Union of Geodesy and Geophysics 1987–1990. American Geophysical Union, Washington, DC, pp. 227–239.

Huyakorn, P.S., Pinder, G.F., 1983. Computational Methods in Subsurface Flow. Academic Press, New York.

Huyakorn, P.S., Thomas, S.D., Thomason, B.M., 1984. Techniques for making finite elements competitive in modeling flow in variably saturated media. Water Resources Research 20, 1099–1115.

Huyakorn, P.S., Panday, S., Wu, Y.S., 1994. A three-dimensional multiphase flow model for assessing NAPL contamination in porous and fractured media: 1. Formulation. Journal of Contaminant Hydrology 16, 109–130.

Istok, J., 1989. Groundwater modeling by the finite element method. American Geophysical Union Water Resources 13.

Kaluarachchi, K., Parker, J., 1989. An efficient finite element method for modeling multiphase flow. Water Resources Research 25 (1), 43–54.

Kuiper, L.K., Illangasekare, T.K., 1998. Numerical simulation of NAPL flow in the subsurface. Computational Geosciences 2, 171–189.

Mercer, J.W.Tr., Faust, C., Pinder, G.F., 1974. Geothermal reservoir simulation. Proceedings of NSF/RANN Conference on Research for the Development of Geothermal Energy Resources. California Institute of Technology, Pasadena, CA, pp. 256–267.

Montazer, P., Wilson, W.E., 1984. Conceptual hydrologic model of flow in the unsaturated zone, Yucca Mountain, Nevada. Water Resources Investigations Report 84-4345. U.S. Geological Survey.

Morel-Seytoux, Billica, J.A., 1985. A two-phase numerical model for prediction of infiltration: application to a semi-infinite soil column. Water Resources Research 21 (4), 607–615.

Narasimhan, T.N., Witherspoon, P.A., 1976. An integrated finite difference method for analyzing fluid flow in porous media. Water Resources Research 12 (1), 57–64.

Palagi, C.L., Aziz, K., 1994. Use of voronoi grid in reservoir simulation. SPE Advanced Technology Series 2 (2), 69–77.

Panday, S., Wu, Y.S., Huyakorn, P.S., Springer, E.P., 1994. A three-dimensional multiphase flow model for assessing NAPL contamination in porous and fractured media: 2. Porous medium simulation examples. Journal of Contaminant Hydrology 16, 131–156.

Parker, J.C., Lenhard, R.J., Kuppusamy, T., 1987. A parametric model for constitutive properties governing multiphase flow in porous media. Water Resources Research 23 (4), 618–624.

Peaceman, D.W., 1977. Fundamentals of numerical reservoir simulation. Developments in Petroleum Sciences, vol. 6. Elsevier, Amsterdam.

Peaceman, D.W., Rachford Jr., H.H., 1962. Numerical calculation of multidimensional miscible displacement. AIME Transactions 225, 327–339.

Pruess, K., 1983. GMINC—A Mesh Generator for Flow Simulations in Fractured Reservoirs, Report LBL-15227, Berkeley, CA: Lawrence Berkeley National Laboratory.

Pruess, K., 1987, TOUGH User's Guide. Nuclear Regulatory Commission, Report NUREG/CR-4645; Report LBL-20700. Berkeley, CA: Lawrence Berkeley National Laboratory.

Pruess, K., 1991. TOUGH2—A General-Purpose Numerical Simulator for Multiphase Fluid and Heat Flow, Report LBL-29400, Lawrence Berkeley National Laboratory, Berkeley, CA.

Pruess, K., Narasimhan, T.N., 1985. A practical method for modeling fluid and heat flow in fractured porous media. Society of Petroleum Engineer Journal 25, 14–26.

Rousseau, J.P., Kwicklis, E.M., Gillies, D.C. (Eds.) 1996. Hydrogeology of the Unsaturated Zone, North Ramp Area of the Exploratory Studies Facility, Yucca Mountain, Nevada. USGS-WRIR-98-4050 Yucca Mountain Project Milestone 3GUP667M, Denver.

Scott, R.B., Bonk, J., 1984. Preliminary geologic map of Yucca Mountain, Nye County, Nevada, with geologic sections. Report USGS OFR-84-494, US Geological Survey.

Thomas, K.L., 1978. Three-dimensional geothermal reservoir simulation. Society of Petroleum Engineer Journal, 144–154, Trans. AIME, Vol. 262.

Thomas, G.W., 1982. Principles of Hydrocarbon Reservoir Simulation. International Human Resources Development, Boston.

Warren, J.E., Root, P.J., 1963. The behavior of naturally fractured reservoirs. Society of Petroleum Engineer Journal, 245–255, Trans. SPE of AIME, Vol. 228.

Wittwer, C., Chen, G., Bodvarsson, G.S., Chornack, M.P., Flint, A.L., Flint, L.E., Kwicklis, E., Spengler, R.W., 1995. Preliminary Development of the LBL/USGS Three-Dimensional Site—Scale Model of Yucca Mountain, Nevada. Report LBL-37356, UC-814, Lawrence Berkeley National Laboratory, Berkeley, CA.

Wu, Y.S., 1998. MSFLOW: Multiphase Subsurface Flow Model of Oil, Gas and Water in Porous and Fractured Media with Water Shut-off Capability, Documentation and User's Guide, Walnut Creek, CA.

Wu, Y.S., 1999. A virtual node method for treatment of wells in modeling multiphase flow in reservoirs. Proceedings of the Twenty-Fourth Workshop, Geothermal Reservoir Engineering, Stanford University, CA, pp. 144–157.

Wu, Y.S., 2000. A virtual node method for handling wellbore boundary conditions in modeling multiphase flow in porous and fractured media. Water Resources Research 36 (3), 807–814.

Wu, Y.S., Pruess, K., 1988. A multiple-porosity method for simulation of naturally fractured petroleum reservoirs. SPE Reservoir Engineering 3, 327–336.

Wu, Y.S., Kool, J., McCord, J., 1992. An Evaluation of Alternative Numerical Formulations for Two-Phase Air Water Flow in Unsaturated Soils. AGU Spring Meeting, Montreal.

Wu, Y.S., Huyakorn, P.S., Park, N.S., 1994. A vertical equilibrium model for assessing nonaqueous phase liquid contamination and remediation of groundwater systems. Water Resources Research 30 (4), 903–912.

Wu, Y.S., Ahlers, C.F., Fraser, P., Simmons, A., Pruess, K., 1996. Software Qualification Of Selected TOUGH2 Modules. Report LBL-39490; UC-800, Lawrence Berkeley National Laboratory, Berkeley, CA.

Wu, Y.S., Forsyth, P.A., Jiang, H., 1996b. A consistent approach for applying numerical boundary conditions for multiphase subsurface flow. Journal of Contaminant Hydrology 23, 157–184.

Wu, Y.S., Ritcey, A.C., Ahlers, C.F., Hinds, J.J., Mishra, A.K., Haukwa, C., Liu, H.H., Sonnenthal, E.L., Bodvarsson, G.S., 1998. 3-D UZ Site-Scale Model for Abstraction in TSPA-VA. Yucca Mountain Project Level 4 Milestone SLX01LB3. Berkeley, CA: Lawrence Berkeley National Laboratory.

Wu, Y.S., Haukwa, C., Bodvarsson, G.S., 1999. A site-scale model for fluid and heat flow in the unsaturated zone of Yucca Mountain, Nevada. Journal of Contaminant Hydrology 38 (1–3), 185–215.